

# A new method to measure the virial factors in the reverberation mapping of AGNs

H. T. Liu<sup>1,3\*</sup>, H. C. Feng<sup>1,2,3</sup> and J. M. Bai<sup>1,3</sup>

<sup>1</sup>Yunnan Observatories, Chinese Academy of Sciences, Kunming, Yunnan 650011, China

<sup>2</sup>University of Chinese Academy of Sciences, Beijing 100049, China

<sup>3</sup>Key Laboratory for the Structure and Evolution of Celestial Objects, Chinese Academy of Sciences, Kunming, Yunnan 650011, China

Accepted . Received

## ABSTRACT

Based on the gravitational redshift, one prediction of Einstein’s general relativity theory, of broad optical emission lines in active galactic nuclei (AGNs), a new method is proposed to estimate the virial factors  $f$  in measuring black hole masses  $M_{\text{RM}}$  by the reverberation mapping of AGNs. The factors  $f$  can be measured on the basis of two physical quantities, i.e. the gravitational redshifts  $z_g$  and full widths at half maxima  $v_{\text{FWHM}}$  of broad lines. In the past it **has been** difficult to determine the factors  $f$  for individual AGNs. **We apply this new method to several** reverberation mapped Seyfert 1 galaxies. There is a correlation between  $f$  and broad-line region (BLR) radius  $r_{\text{BLR}}$ ,  $f = 5.4r_{\text{BLR}}^{0.3}$ , for the gravitationally redshifted broad lines He II, He I, H $\beta$  and H $\alpha$  in narrow-line Seyfert 1 galaxy (NLS1) Mrk 110. This correlation results from the radiation pressure influence of **the** accretion disc on the BLR clouds. The radiation pressure influence seems to be more important than usually thought in AGNs. Mrk 110 has  $f \approx 8\text{--}16$ , distinctly larger than the mean  $\langle f \rangle \approx 1$ , usually used to estimate  $M_{\text{RM}}$  in the case of  $v_{\text{FWHM}}$ . NGC 4593 and NLS1 Mrk 486 has  $f \approx 3$  and  $f \approx 9$ , respectively. Higher  $f$  **values** of several tens are derived for **three other** NLS1s. There is a correlation between  $f$  and accretion rate  $\dot{M}_{f=1}$ ,  $f = 6.8\dot{M}_{f=1}^{0.4}$  for five objects, where  $\dot{M}_{f=1} = \dot{M}_{\bullet}/L_{\text{Edd}}c^{-2}$  **as  $f = 1$  is assumed to estimate  $M_{\text{RM}}$  used in the Eddington luminosity  $L_{\text{Edd}}$ ,  $\dot{M}_{\bullet}$  is the mass accretion rate, and  $c$  is the speed of light. These larger  $f$  values will produce higher  $M_{\text{RM}}$  values and lower Eddington ratios.**

**Key words:** black hole physics – galaxies: active – galaxies: nuclei – galaxies: Seyfert – quasars: emission lines.

## 1 INTRODUCTION

Active galactic nuclei (AGNs), such as quasars and Seyfert galaxies, can be powered by the **release** of gravitational potential energy of matter accreted onto supermassive black holes surrounded by accretion discs (Rees et al. 1982; Rees 1984). The reverberation mapping (RM) model shows that the broad emission line variations are driven by the ionizing continuum variations through the photoionization process (e.g. Blandford & McKee 1982; Peterson 1993). Broad-line region (BLR) radius  $r_{\text{BLR}}$  can be determined by **the** time lag  $\tau$  between the broad-line and continuum variations, as  $r_{\text{BLR}} = \tau c$ , where  $c$  is the speed of light. The RM observations and researches have been carried out for AGNs over the last several decades (e.g. Kaspi & Netzer 1999; Kaspi et al. 2000, 2007; Peterson et al. 2005; Denney et al.

2010; Haas et al. 2011; Pozo Nuñez et al. 2012; Du et al. 2014, 2015; Pei et al. 2014; Wang et al. 2014; Barth et al. 2015; Hu et al. 2015). Recently, some RM surveys **have been** proposed and carried out, such as the Sloan Digital Sky Survey (SDSS) spectroscopic RM project (Shen et al. 2015a,b, 2016) and the OzDES AGN spectroscopic RM project (King et al. 2015). **These RM studies will be the most efficient method to accurately estimate black hole masses  $M_{\text{RM}}$  of AGNs at moderate-to-high redshifts.  $M_{\text{RM}}$  is given by  $M_{\text{RM}} = f v_{\text{FWHM}}^2 r_{\text{BLR}} / G$ , where  $f$  is the virial factors,  $v_{\text{FWHM}}$  is the full widths at half maxima of emission lines and  $G$  is the gravitational constant (Peterson et al. 2004).** However, the virial factors  $f$  in the  $M_{\text{RM}}$  estimates are uncertain due to the unclear kinematics and geometry of BLRs in AGNs (Peterson et al. 2004; Woo et al. 2015). An average  $\langle f \rangle \approx 1$  is derived by the black hole mass–stellar velocity dispersion ( $M_{\bullet} - \sigma_{\star}$ ) relation for the low redshift quiescent galaxies and/or rever-

\* E-mail: htliu@ynao.ac.cn

beration mapped AGNs using  $v_{\text{FWHM}}$  of Balmer emission lines (Onken et al. 2004; Piotrovich et al. 2015; Woo et al. 2015). Constraining the virial factors  $f$  is an important task for investigating black hole mass related issues.

The BLR cloud motions of the reverberation mapped AGNs are believed or assumed to be dominated by the gravitational forces of the central supermassive black holes (i.e. virialized motions) (e.g. Krolik et al. 1991; Wandel et al. 1999; Krolik 2001; Barth et al. 2011; Du et al. 2014; Wang et al. 2014). The virialized motions generate the observed  $v_{\text{FWHM}}$  of optical broad emission lines, typically thousands of  $\text{km s}^{-1}$ . The optical BLRs usually span over distances of hundreds to thousands of the gravitational radii from the **central** black holes for the reverberation mapped AGNs. **Despite** the huge distances, the broad lines should be redshifted by the central black hole's gravity. Gravitational redshift in the weak field regime establishes pure shifts of spectral features without changing their intrinsic shapes and in the strong field regime produces remarkable distortions of spectral shapes (Müller & Wold 2006). Remarkable profile distortion is a key feature of relativistic spectra in AGNs with very skewed and asymmetric line profiles, e.g. iron  $\text{K}\alpha$  lines, generated in the emitting regions very close to the central black holes (e.g. Fabian et al. 1989; Popovic et al. 1995; Tanaka et al. 1995; Fabian et al. 2000; Reynolds & Nowak 2003). **In the literature**, there are three ways to measure the gravitational redshift  $z_g$ . First, it is measured for a broad line as a redshift difference with respect to **narrow emission lines like**  $[\text{O III}] \lambda 5007$  (e.g. Zheng & Sulentic 1990; McIntosh et al. 1999b; Tremaine et al. 2014). Second, it is measured at different levels of the line intensity as a centroid shift with respect to the broad line peak, eliminating all spectra with blueshifted profiles (Jonić et al. 2016). Third, it is measured as a broad-line center shift of the root mean square (rms) spectrum with respect to the narrow line (Kollatschny 2003b). A sign of  $z_g$  was found in a statistical sense for broad  $\text{H}\beta$  in the single-epoch spectra of over 20,000 quasars in the SDSS Data Release 7 (DR7) (Tremaine et al. 2014). Jonić et al. (2016) found **a positive correlation between intrinsic redshift  $\Delta z_{50}$ , dominantly caused by the gravitational effect, and  $v_{\text{FWHM}}$  of  $\text{H}\beta$  for 209 AGNs taken from the SDSS DR7, which matches the theoretically expected relationship of  $\Delta z_{50} \propto v_{\text{FWHM}}^2$** . The redshifts of the rms profiles of broad lines and the BLR radii in Mrk 110 also follow the gravitational redshift prediction (see Fig. 3 in Kollatschny 2003b).

The RM masses of the black holes are  $M_{\text{RM}} \sim 10^6 - 10^7 M_{\odot}$  for Seyfert 1 galaxies (e.g. Kaspi & Netzer 1999; Kaspi et al. 2000; Peterson et al. 2005; Bentz et al. 2006; Denney et al. 2010; Haas et al. 2011; Du et al. 2014, 2015; Wang et al. 2014). Seyfert 1 galaxies have a relatively high Eddington ratio  $L_{\text{bol}}/L_{\text{Edd}}$ , where  $L_{\text{bol}}$  is the bolometric luminosity and  $L_{\text{Edd}}$  is the Eddington luminosity. Narrow-line Seyfert 1 galaxies (NLS1s) seem to have a **higher** Eddington ratio. Some NLS1s **appear to be accreting at super-Eddington rates**. A large RM campaign was performed by the Yunnan Observatory 2.4 m telescope from 2012 to 2013 for AGNs with super-Eddington accreting massive black holes (SEAMBHs) (Du et al. 2014; Wang et al. 2014). Hu et al. (2015) studied the properties of emission lines for 10 NLS1s with SEAMBHs, and found the red-

shifts and/or blueshifts of  $\text{H}\beta$  and  $\text{Fe II}$ . The inflow and outflow of BLR gas may generate redshifts and blueshifts, respectively. Kollatschny (2003a) ruled out that radial inflow or outflow motions are dominant in the BLR of NLS1 Mrk 110. Kollatschny (2003b) found the gravitationally redshifted broad emission lines  $\text{He II}$ ,  $\text{He I}$ ,  $\text{H}\beta$  and  $\text{H}\alpha$ . The BLRs will **"breathe"** with the central radiation variations (e.g. Barth et al. 2015, references therein). The breaths occur on short timescales of days to weeks in response to continuum variations, and the broad-line shifts of  $\sim 100 \text{ km s}^{-1}$  were found over about one month. The breathing effects of BLRs on the broad-line shifts might be eliminated in the **rms and mean spectra of the reverberation mapped AGNs by virtue of averaging over many breaths, and this was the approach employed in Mrk 110 by Kollatschny (2003b)**. The redshifted  $\text{H}\alpha$  and  $\text{H}\beta$  broad lines were found with the rms spectra for Seyfert 1 galaxy NGC 4593, and their redward shifts might be interpreted as the gravitational redshift (Kollatschny & Dietrich 1997).

**In this paper, we derive a new method to estimate the virial factors  $f$  with the gravitationally redshifted broad optical emission lines in AGNs, and apply this new method to several reverberation mapped Seyfert 1 galaxies.** The structure of this paper is as follows. Section 2 presents the method. Section 3 describes the application to Mrk 110. Section 4 is for the application to NGC 4593. Section 5 is for the applications to Mrk 493, *IRAS* 04416 and Mrk 42. Section 6 presents discussion and conclusions. Throughout this paper, we use the standard cosmology with  $H_0 = 70 \text{ km s}^{-1} \text{ Mpc}^{-1}$ ,  $\Omega_{\text{M}} = 0.3$ , and  $\Omega_{\Lambda} = 0.7$  (Spergel et al. 2003; Riess et al. 2004).

## 2 METHOD

The BLRs are distant from the central black holes for the reverberation mapped AGNs. The Schwarzschild metric will be reasonable to describe the space-time around the BLRs. The Kerr metric and the Schwarzschild metric have the identical effect on the gravitational redshift at distances larger than about one hundred gravitational radii from the black holes (see Fig. 9 in Müller & Wold 2006). The Schwarzschild space-time is

$$\begin{aligned} ds^2 &= -g_{\mu\nu} dx^\mu dx^\nu \\ &= \left(1 - \frac{2GM_\bullet}{c^2 r}\right) c^2 dt^2 - \left(1 - \frac{2GM_\bullet}{c^2 r}\right)^{-1} dr^2 \\ &\quad - r^2 d\theta^2 - r^2 \sin^2 \theta d\varphi^2, \end{aligned} \quad (1)$$

where  $G$  is the gravitational constant and  $M_\bullet$  is black hole mass. The ratio of the frequency of atomic transition  $\nu_e$  at the BLR radius  $r_{\text{BLR}}$  to the frequency  $\nu_o$  observed at infinite distance is (static cloud)

$$\begin{aligned} \frac{\nu_o}{\nu_e} &= \frac{(-g_{00})_{r_{\text{BLR}}}^{1/2}}{(-g_{00})_{\infty}^{1/2} c} \\ &= \left(1 - \frac{2GM_\bullet}{c^2 r_{\text{BLR}}}\right)^{1/2}, \end{aligned} \quad (2)$$

where  $(-g_{00})_{\infty} = 1$  at the observer's frame. So, the gravitational redshift is

$$z_g = \frac{\nu_e}{\nu_o} - 1 = \left(1 - \frac{2GM_{\bullet}}{c^2 r_{\text{BLR}}}\right)^{-1/2} - 1. \quad (3)$$

The black hole mass  $M_{\bullet}$  is

$$M_{\bullet} = \frac{1}{2} G^{-1} c^2 r_{\text{BLR}} [1 - (1 + z_g)^{-2}], \quad (4)$$

and the first order approximation is

$$M_{\bullet} \cong G^{-1} c^2 z_g r_{\text{BLR}}, \quad (5)$$

if  $z_g \ll 1$ . Equation (5) was used to estimate  $M_{\bullet}$  in Kollatschny (2003b) and Zheng & Sulentic (1990).

In general, the gravitational redshift  $z_g$  is derived from the redshift difference of the broad emission lines relative to the narrow emission lines. **When** the narrow lines do not appear in the spectrum containing the broad lines, the redshift difference  $\Delta z_{i,j} = z_i - z_j = z_{g,i} - z_{g,j}$  for the broad lines  $i$  and  $j$  **can be** used to estimate  $M_{\bullet}$ . Hence we have

$$\begin{aligned} \Delta z_{i,j} &= \left(1 - \frac{2GM_{\bullet}}{c^2 r_{\text{BLR},i}}\right)^{-1/2} - \left(1 - \frac{2GM_{\bullet}}{c^2 r_{\text{BLR},j}}\right)^{-1/2} \\ &\cong \frac{GM_{\bullet}}{c^2} \left(\frac{1}{r_{\text{BLR},i}} - \frac{1}{r_{\text{BLR},j}}\right), \end{aligned} \quad (6)$$

where  $r_{\text{BLR}} \gg r_g = GM_{\bullet}/c^2$  ( $r_g$  is the gravitational radius). And then we have

$$M_{\bullet} \cong G^{-1} c^2 \Delta z_{i,j} \left(\frac{1}{r_{\text{BLR},i}} - \frac{1}{r_{\text{BLR},j}}\right)^{-1}, \quad (7)$$

where  $r_{\text{BLR},i}$  and  $r_{\text{BLR},j}$  correspond to the broad lines  $i$  and  $j$ , respectively.  $M_{\bullet}$  can be measured by the virial theorem for the reverberation mapped AGNs (Peterson et al. 2004):

$$M_{\text{RM}} = f \frac{v_{\text{FWHM}}^2 r_{\text{BLR}}}{G}. \quad (8)$$

If the RM method and the gravitational redshift method give the same mass  $M_{\bullet}$ , we have the virial factor

$$f = \frac{1}{2} \frac{c^2}{v_{\text{FWHM}}^2} [1 - (1 + z_g)^{-2}], \quad (9)$$

for the reverberation mapped AGNs. This gravitational redshift approach will be a **simple and direct** method to estimate the virial factor  $f$  in equation (8). If  $f$  is fully generated by the oblique effect of a **disc-like BLR** with inclinations  $\theta$ ,  $f = 1/4 \sin^2 \theta$  (McLure & Dunlop 2001). **For**  $f = 1$ ,  $\theta = 30$  degrees. Hereafter,  $M_{\text{grav}}$  denotes  $M_{\bullet}$  estimated by equations (4), (5) and (7), and  $M_{\text{RM}}$  denotes  $M_{\bullet}$  estimated by equation (8).

### 3 APPLICATION TO MRK 110

The shifts of the rms line centers (uppermost 20%) with respect to the narrow lines are identified as the gravitational redshifts (Kollatschny 2003b). The mean profiles of the broad lines are not shifted with respect to the forbidden narrow lines on the other hand. Therefore, the differential shifts of the rms profiles with respect to the narrow lines are identical to their shifts with respect to the mean

profiles (Kollatschny 2003b). The virial factors  $f$  are derived by equation (9) for the broad lines He II, He I, H $\beta$  and H $\alpha$  (see Table 1). Considering the errors of  $v_{\text{FWHM}}$  and  $z_g$ , the  $f$  distribution is generated with equation (9) by  $10^4$  realizations of Monte Carlo simulation. The mean and standard deviation of this distribution are regarded as the expectation and uncertainty of  $f$ , respectively. The helium and hydrogen lines have  $f \approx 8$ –16 that are larger than the average  $\langle f \rangle \approx 1$  usually accepted for the reverberation mapped AGNs. These  $f$  values of the helium lines are slightly smaller than those of the hydrogen lines. If  $f$  is fully generated by the oblique effect of the disc-like BLRs,  $\theta \approx 7$ –10 degrees (see Table 1), which confirm the nearly face-on view of accretion disc in Mrk 110 suggested by Kollatschny (2003a,b). The broad lines He II, He I, H $\beta$  and H $\alpha$  have obvious stratification in the BLRs, as predicted by the virial theorem (Kollatschny 2003b), and **arise from increasing distances** from the central black hole. These stratification BLRs are dominated by the central supermassive black hole's gravity. Mrk 110 will have the virial velocity  $v_c^2 = GM_{\bullet} r_{\text{BLR}}^{-1}$  and  $v_{\text{FWHM}}^2 \propto v_c^2 \propto r_{\text{BLR}}^{-1}$ . We have  $f \cong z_g c^2 / v_{\text{FWHM}}^2$  because  $z_g \ll 1$  in equation (9) for Mrk 110, and then  $f \propto z_g r_{\text{BLR}} \propto M_{\bullet}$  (see equation [5]).  $M_{\bullet}$  can be regarded as a constant in observation periods for individual AGNs. So,  $f$  **should be** independent of  $r_{\text{BLR}}$ . However, there is a positive correlation between  $f$  and  $r_{\text{BLR}}$  for Mrk 110,

$$\log f = 0.73(\pm 0.08) + 0.30(\pm 0.07) \times \log r_{\text{BLR}} \quad (10)$$

**with a Pearson's correlation coefficient  $r = 0.948$  at the confidence level of 94.8 percent. The "FITEXY" estimator (Press et al. 1992) gives  $\log f = 0.74(\pm 0.21) + 0.29(\pm 0.22) \times \log r_{\text{BLR}}$  for the data and uncertainties in x and y with a chi-square  $\chi^2 = 0.180$  and a goodness-of-fit  $Q = 0.914$  (see Figure 1). These two best fit lines are indistinguishable.** This correlation of  $f = 5.4(\pm 1.0) \times r_{\text{BLR}}^{0.3 \pm 0.1}$  is inconsistent with the independent prediction of the virial theorem.

There are two paths to estimate  $M_{\bullet}$ , i.e. the single broad-line estimation (equation [4]) and the broad-line-to-broad-line comparison (equation [7]). The gravitational masses  $M_{\text{grav}}$  are estimated for the broad lines He II, He I, H $\beta$  and H $\alpha$  (see Tables 1 and 2). According to basic error propagation conventionally used in the RM method, we estimate the uncertainty of  $M_{\text{grav}}$  from the errors of  $r_{\text{BLR}}$  and  $z_g$ . Each  $M_{\text{grav}}$  in Table 2 will correspond to two  $M_{\text{grav}}$  in Table 1, because equation (7) is based on two broad lines. Comparisons show that the masses estimated by these two paths are consistent with each other (see Figure 2). This agreement indicates that the broad-line-to-broad-line comparison path is feasible and reliable to estimate  $M_{\bullet}$ . The black hole masses in Tables 1 and 2 are also consistent with the mean mass of  $\log M_{\text{grav}}/M_{\odot} = 8.15$  derived in Kollatschny (2003b). The broad-line-to-broad-line comparison path **avoids any potential difficulty coming from blueshifts of narrow [O III]  $\lambda 5007$  in the single broad-line path. Such narrow line blueshifts would** equivalently generate the broad line redshift when the blueshifted narrow line is used as the reference to estimate  $z_g$ . In principle, the broad-line-to-broad-line comparison path could mostly eliminate the line shift influence due to the BLR "breath". The broad-line-to-broad-line comparison path seems to be better than the single broad-

**Table 1.** The details of  $v_{\text{FWHM}}$ ,  $z_g$ ,  $\tau$ ,  $M_{\text{grav}}$ ,  $f$  and  $\theta$  for Mrk 110 and NGC 4593

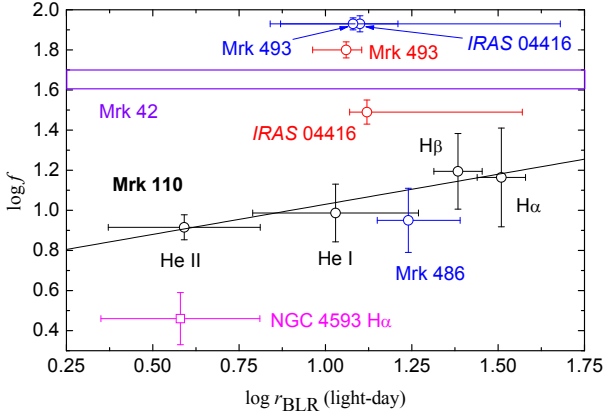
Object	Line	$\frac{v_{\text{FWHM}}}{\text{km s}^{-1}}$	$z_g$	$\tau$ (days)	$\log \frac{M_{\text{grav}}}{M_{\odot}}$	$f$	$\theta^\circ$
(1)	(2)	(3)	(4)	(5)	(6)	(7)	(8)
Mrk 110	He II $\lambda 4686$	$4444 \pm 200$	$0.00180 \pm 0.00020$	$3.9 \pm 2$	$8.09 \pm 0.23$	$8.23 \pm 1.18$	$10.12 \pm 0.74$
Mrk 110	He I $\lambda 5876$	$2404 \pm 100$	$0.00062 \pm 0.00020$	$10.7 \pm 6$	$8.07 \pm 0.28$	$9.70 \pm 3.21$	$9.24 \pm 1.56$
Mrk 110	H $\beta$ $\lambda 4861$	$1515 \pm 100$	$0.00039 \pm 0.00017$	$24.2 \pm 4$	$8.22 \pm 0.20$	$15.65 \pm 6.79$	$7.26 \pm 1.68$
Mrk 110	H $\alpha$ $\lambda 6563$	$1315 \pm 100$	$0.00025 \pm 0.00017$	$32.3 \pm 5$	$8.15 \pm 0.30$	$14.59 \pm 8.27$	$7.52 \pm 2.79$
NGC 4593	H $\alpha$ $\lambda 6563$	$3400 \pm 200$	$0.00037 \pm 0.00010$	$3.8 \pm 2.0$	$7.39 \pm 0.26$	$2.91 \pm 0.86$	$17.04 \pm 2.60$

Notes: Column 1: object names; Column 2: emission line names; Column 3:  $v_{\text{FWHM}}$  of broad lines in the rms spectra; Column 4: the gravitational redshifts; Column 5: time lags of lines in the rest frame; Column 6: the gravitational masses derived from equation (4); Column 7: the virial factors; Column 8: inclinations if  $f$  is fully generated by the inclination effect of the disc-like BLRs.

**Table 2.**  $M_{\text{grav}}$  given by broad line pairs for Mrk 110

Line	He I $\lambda 5876$	H $\beta$ $\lambda 4861$	H $\alpha$ $\lambda 6563$
(1)	(2)	(3)	(4)
He II $\lambda 4686$	$8.10 \pm 0.39$	$8.06 \pm 0.28$	$8.08 \pm 0.26$
He I $\lambda 5876$		$7.89 \pm 0.66$	$8.02 \pm 0.48$
H $\beta$ $\lambda 4861$			$8.38 \pm 0.82$

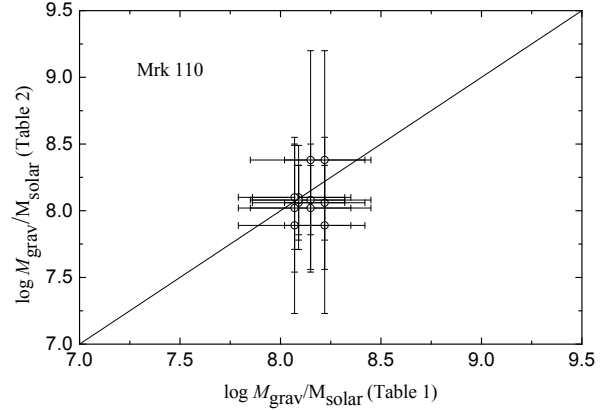
Notes: the gravitational masses are derived from equation (7) and scaled as  $\log \frac{M_{\text{grav}}}{M_{\odot}}$ .

**Figure 1.**  $\log f$  vs  $\log r_{\text{BLR}}$ . Black circles are for Mrk 110. Circles in color are for SEAMBH AGNs. Red circles denote the H $\beta$  line, and blue circles denote the Fe II line. Violet lines denote the  $f$  values for Mrk 42. Black line is the best fit line to the black circles.

line path to estimate  $M_{\bullet}$  when there are several broad lines in the spectrum. So, equation (7) is appropriate to estimate  $M_{\bullet}$  for multi-broad-line AGNs. Equation (4) is appropriate for a single broad line except for the blueshift issue of the narrow line used as the reference to estimate  $z_g$ .

#### 4 APPLICATION TO NGC 4593

NGC 4593 is a nearby Seyfert 1 galaxy. This object is a sub-Eddington accreting AGN with an average  $\dot{M} = 0.08$ , where  $\dot{M} = \dot{M}_{\bullet}/L_{\text{Edd}}c^{-2}$  is the dimensionless accretion rate and  $\dot{M}_{\bullet}$  is the mass accretion rate (Du et al. 2015). **Hereafter,  $\dot{M}$  is denoted by  $\dot{M}_{f=1}$ , because its calculation is assuming  $f = 1$  to estimate  $M_{\text{RM}}$  used in  $L_{\text{Edd}}$ .** Early RMs yielded a lag of four days indicating a very compact BLR (Dietrich et al. 1994). Recent RMs con-

**Figure 2.** Comparison between  $M_{\text{grav}}$  derived from equations (4) and (7). Black line is  $y = x$ .

firm this lag of four days (e.g. Du et al. 2015, references therein). Kollatschny & Dietrich (1997) found the redshifted H $\alpha$  and H $\beta$  broad lines with the rms spectra, and thought that the observed redshift might be interpreted as the gravitational redshift. The central component of H $\alpha$  is redshifted by  $110 \pm 30 \text{ km s}^{-1}$  with respect to the narrow line, and the H $\beta$  rms spectrum shows a redshift of the same order of magnitude. We have  $v_{\text{FWHM}} = 3400 \pm 200 \text{ km s}^{-1}$  for both of the H $\alpha$  rms and mean spectra. The relevant physical quantities of H $\alpha$  are listed in Table 1.  $M_{\text{grav}} = 2.5(\pm 1.5) \times 10^7 M_{\odot}$  is given by equation (4).  $f = 2.9$  is given by the redshifted H $\alpha$  line. This  $f$  value is slightly higher than  $\langle f \rangle \approx 1$ , and is smaller than those of Mrk 110.

In plot of  $\log f$  versus  $\log r_{\text{BLR}}$ , NGC 4593 is below the best fit line to Mrk 110 (see Figure 1). If  $f$  is fully generated by the inclination effect of the BLR for NGC 4593,  $\theta \approx 17$  degrees. The inclination effect will generate different  $f$  even for the same BLR (e.g. McLure & Dunlop 2001). Another possible explanation of the different  $f$  is that the accretion rate  $\dot{M}_{f=1}$  dominates the factor  $f$ , because  $f = 2.9$  and  $\dot{M}_{f=1} = 0.08$  in NGC 4593 are smaller than  $f = 14.6$  and  $\dot{M}_{f=1} = 5.89$  (Du et al. 2015) in Mrk 110 for H $\alpha$ , respectively. A new quantity  $\dot{M}_f$  is defined as a normalization of  $\dot{M}$  relative to  $f$ .  $\dot{M}_f$  corrects the underestimation of  $M_{\text{RM}}$  due to the use of  $f = 1$ , takes into account differences in the  $\dot{M}$  estimates, and represents the more realistic dimensionless accretion rate. NGC 4593 and Mrk 110 have  $\dot{M}_f = 0.03$  and 0.40 for H $\alpha$ , respectively. The normalized value  $\dot{M}_f$  reflects the composite effect of the central black hole's gravity, the

central radiation pressure and the kinematics and geometry of BLR. Mrk 110 has higher  $\dot{M}_f$  and  $f$  than NGC 4593.

## 5 APPLICATIONS TO MRK 493, IRAS 04416 AND MRK 42

Hu et al. (2015) studied the properties of emission lines for 10 NLS1s. Mrk 493, IRAS 04416+1215 and Mrk 42 have the redward shifted optical Fe II and H $\beta$  lines with respect to [O III]  $\lambda$ 5007. The virialized motions of BLR clouds are assumed to estimate  $M_{\text{RM}}$  in the RM of H $\beta$  for these NLS1s (Du et al. 2014; Wang et al. 2014). The redward shifts of H $\beta$  and Fe II may be the gravitational redshifts. The Fe II lag is consistent with the H $\beta$  lag for the same source (see Table 3). Mrk 493 and Mrk 42 have the Fe II  $v_{\text{FWHM}}$  indistinguishable from the H $\beta$   $v_{\text{FWHM}}$ . The Fe II  $v_{\text{FWHM}}$  is slightly smaller than the H $\beta$   $v_{\text{FWHM}}$  in IRAS 04416. There are no obvious stratification **for these two emission lines** in the BLRs for Mrk 493, IRAS 04416 and Mrk 42. Here, we regard these redward shifts of the Fe II and H $\beta$  lines as the gravitational redshifts. The details for these three NLS1s are listed in Table 3. The factors  $f$  and the masses  $M_{\text{grav}}$  are estimated by equations (9) and (4), respectively. These three NLS1s have higher  $f$  than Mrk 110 (see Figure 1). Their  $f$  values are much larger than  $\langle f \rangle \approx 1$ , **implying larger black hole masses than typically estimated from  $M_{\text{RM}}$** . The higher masses will decrease the Eddington ratios. These results are very similar to those of Mrk 110 with a mean  $f \approx 12$ , which makes  $M_{\text{RM}}$  increase by an order of magnitude.

These three NLS1s and Mrk 110 have comparable  $r_{\text{BLR}}$  and  $M_{\text{grav}}$ , but distinctly different  $f$  (see Figure 1). These behaviors may be from the difference of accretion states. Mrk 493 and IRAS 04416 have  $\dot{M}_{f=1} = 75.9$  and  $\dot{M}_{f=1} = 426.6$ , respectively (Du et al. 2015). Mrk 493 and IRAS 04416 have a mean  $f = 73.3$  and  $f = 58.7$ , respectively. Thus, Mrk 493 and IRAS 04416 have  $\dot{M}_f = 1.04$  and  $\dot{M}_f = 7.27$ , respectively. Mrk 110 has a mean  $f = 12.0$  and  $\dot{M}_f = 0.49$ . In terms of  $\dot{M}_{f=1}$  and  $\dot{M}_f$ , Mrk 493 and IRAS 04416 are at higher accretion states than Mrk 110. The higher accretion rate seems to result in the larger  $f$ . **The higher accretion rate will result in stronger radiation pressure on the BLR clouds.** The higher radiation pressure will counteract a **greater** proportion of the black hole's gravity, and then the BLR clouds will have a smaller virial velocity, i.e.  $v_{\text{FWHM}}$  will decrease if the radiation pressure increases, given that the BLR clouds are in virialized motions. Ultimately, the radiation pressure will influence  $M_{\text{RM}}$ . Thus, the factors  $f$  given by equation (9) will be higher than expected from the virial assumption without considering the radiation pressure.

A higher mass  $\log M_{\text{grav}}/M_{\odot} \approx 9.5$  is estimated by equation (7) for IRAS 04416. A very large error of  $\log M_{\text{grav}}/M_{\odot}$  will be generated by the larger error of  $\tau$  ( $r_{\text{BLR}} = c\tau$ ) (see Table 3). This larger mass is on the same order of magnitude as the mass estimated by equation (4) for Fe II when considering its errors. This means that the single broad-line path and the broad-line-to-broad-line comparison path are equally applicable to estimating  $M_{\bullet}$  for IRAS 04416. A further test is needed in the future with high quality time lags of H $\beta$  and Fe II to check the validity of these two paths. The current results indicate that the redward shifts

of H $\beta$  and Fe II with respect to [O III] are reliable to be used as the gravitational redshifts, i.e. the [O III] redshift may be regarded as the systemic redshift. Equation (7) cannot be applied to Mrk 493. The applications to Mrk 110 and IRAS 04416 show that the broad-line-to-broad-line comparison path is more applicable to those AGNs with obvious stratification in the BLRs, such as Mrk 110.

## 6 DISCUSSION AND CONCLUSIONS

The gravitational redshift effect will exist in the broad lines as long as the BLRs surround the central supermassive black holes. However, this gravitational effect is not always observable due to several factors. The first factor is the observational accuracies, such as the low signal to noise ratios. The second is the breathing of BLRs that shifts the broad lines redward or blueward. The rms and mean spectra may eliminate the breathing effect of BLRs on  $z_g$ . The  $z_g$  and  $r_{\text{BLR}}$  of broad lines follow the gravitational redshift prediction in Mrk 110 (see Fig. 3 in Kollatschny 2003b), indicating that the broad line shifts are dominated by the gravitational redshifts for the rms spectra. The rms spectra were used to measure  $z_g$  of the broad lines in Mrk 110 (Kollatschny 2003b) and NGC 4593 (Kollatschny & Dietrich 1997). The third is that the inflow may also produce the broad line redshifts relative to the narrow lines. The RM method assumes that the BLR cloud motions meet the virial theorem. It was ruled out that radial inflow or outflow motions are dominant in the BLRs of NGC 4593 (Kollatschny & Dietrich 1997), Mrk 110 (Kollatschny 2003a), Mrk 50 (Barth et al. 2011) and Mrk 1044 (Du et al. 2016). The fourth is the other broad and/or narrow lines blended with the target broad line. These blended components will influence the  $v_{\text{FWHM}}$  and centroids of broad lines in the rms spectra (e.g. Barth et al. 2015), and may make it difficult to measure  $z_g$ .

Jonić et al. (2016) eliminated all spectra with the blueshifted profiles. Some other effects (e.g. outflows) could be more dominant than the gravitational effects in these spectra, which are not convenient for the researches on  $z_g$ . It is difficult to state that all spectra with strong outflow influence are completely eliminated, since the possible combination of the outflows and the gravitational effects generates symmetrical line shape (Jonić et al. 2016). Their sample number is about 1% of that in Tremaine et al. (2014). So, it is difficult to measure  $z_g$  due to some other effects, and the chance of finding  $z_g$  is very low. The applications may be influenced by the possible combination. The broad-line-to-broad-line comparison path may mostly eliminate the underlying effects (inflows or outflows) by the using of different broad lines rather than a single broad line. These masses derived from equations (4) and (7) for Mrk 110 are consistent with each other within the uncertainties (see Figure 2). For IRAS 04416, these masses given by equation (7) are larger than those given by equation (4), but they are on the same order of magnitude considering the uncertainties. This implies that the underlying effects are notable, but weaker than the gravitational redshift effect for IRAS 04416, and should be mostly eliminated by equation (7). Though, equations (4), (5) and (9) are not applicable to the blueshifted lines (the blueshift is not eliminated for the single broad line), equation (7) may be applicable. NLS1 Mrk 486 has

**Table 3.** The details of  $v_{\text{FWHM}}$ ,  $z_g$ ,  $\tau$ ,  $M_{\text{grav}}$ ,  $f$  and  $\theta$  of NLS1s for the H $\beta$  and Fe II lines

Object	Line	$\frac{v_{\text{FWHM}}}{\text{km s}^{-1}}$	$z_g$	$\tau$ (days)	$\log \frac{M_{\text{grav}}}{M_{\odot}}$	$f$	$\theta^\circ$
(1)	(2)	(3)	(4)	(5)	(6)	(7)	(8)
<i>IRAS</i> 04416+1215	H $\beta$	1522 $\pm$ 44	0.00080 $\pm$ 0.00010	13.3 $^{+13.9}_{-1.4}$	8.27 $^{+0.46}_{-0.07}$	31.14 $\pm$ 4.29	5.14 $\pm$ 0.37
Mrk 42	H $\beta$	802 $\pm$ 18	0.00029 $\pm$ 0.00006			40.60 $\pm$ 8.60	4.50 $\pm$ 0.55
Mrk 493	H $\beta$	778 $\pm$ 12	0.00042 $\pm$ 0.00004	11.6 $^{+1.2}_{-2.6}$	7.93 $^{+0.06}_{-0.11}$	62.44 $\pm$ 6.26	3.63 $\pm$ 0.19
Mrk 486	H $\beta$	1942 $\pm$ 67	-0.00015 $\pm$ 0.00003	23.7 $^{+7.5}_{-2.7}$			
<i>IRAS</i> 04416+1215	Fe II	1313 $\pm$ 50	0.00165 $\pm$ 0.00007	12.6 $^{+16.7}_{-6.7}$	8.56 $^{+0.58}_{-0.23}$	86.31 $\pm$ 7.56	3.09 $\pm$ 0.14
Mrk 42	Fe II	787 $\pm$ 16	0.00035 $\pm$ 0.00006			50.94 $\pm$ 8.97	4.02 $\pm$ 0.38
Mrk 493	Fe II	780 $\pm$ 9	0.00057 $\pm$ 0.00003	11.9 $^{+3.6}_{-6.5}$	8.08 $^{+0.13}_{-0.24}$	84.25 $\pm$ 4.85	3.12 $\pm$ 0.09
Mrk 486	Fe II	1790 $\pm$ 88	0.00032 $\pm$ 0.00011	17.3 $^{+5.8}_{-3.7}$	7.99 $^{+0.21}_{-0.18}$	8.98 $\pm$ 3.21	9.60 $\pm$ 1.73

Notes: Same as in Table 1 except for Column 3: the H $\beta$   $v_{\text{FWHM}}$  from the mean spectra, and the Fe II  $v_{\text{FWHM}}$  given by the mean and standard deviation obtained from the measurements of individual-night spectra (Hu et al. 2015).

the redshifted Fe II broad line (redshifted on  $\pm 1\sigma$ ) and the blueshifted H $\beta$  broad line (blueshifted on  $\pm 1\sigma$ ) (see Table 2 in Hu et al. 2015). Mrk 486 has  $\log M_{\text{grav}}/M_{\odot} = 8.72^{+0.66}_{-0.38}$  given by equation (7) for Fe II and H $\beta$ , and  $\log M_{\text{grav}}/M_{\odot} = 7.99^{+0.21}_{-0.18}$  given by equation (4) for Fe II. These two masses are on the same order of magnitude. The outflow effect may be not strong, but more notable relative to the gravitational redshift effect in Mrk 486.  $f \approx 9$  is estimated by Fe II for Mrk 486 (see Table 3). This value might be the lower limit of  $f$ , for that the redshifted Fe II may not be purely due to the gravitational redshift effect.

In the absence of the radiation pressure on the BLR clouds of AGNs with  $M_{\bullet}$ , there is  $v_c^2 = GM_{\bullet}/r_{\text{BLR}} = r_{\text{BLR}}^{-1}(r_g)c^2$ , where  $r_{\text{BLR}}(r_g)$  is in units of  $r_g$ . At the same time,  $v_{\text{FWHM}}^2 \propto v_c^2 \propto r_{\text{BLR}}^{-1}(r_g)$ . Equations (4) and (9) are combined to give  $f = GM_{\bullet}/(r_{\text{BLR}}v_{\text{FWHM}}^2) \propto r_{\text{BLR}}^{-1}(r_g)/v_{\text{FWHM}}^2 \propto C$ , where  $C$  is independent of  $r_{\text{BLR}}$  and  $M_{\bullet}$ . However, we found in Mrk 110 that  $f = 5.4r_{\text{BLR}}^{0.3}$  (see Figure 1). This discrepancy may result from having ignored the radiation pressure from the accretion disc on the BLR clouds. The radiation pressure will push these clouds towards the larger radius, compared to that in the absence of the radiation pressure. The influence of radiation pressure on RM was studied in depth by Marconi et al. (2008), in which the absorption of ionizing photons and the scattering of nonionizing photons are combined to generate the radiation pressure for NLS1s. After the radiation pressure correction, NLS1s have large black hole masses similar to other broad-line AGNs and follow the same  $M_{\bullet} - \sigma_*$  relation as other active and normal galaxies (Marconi et al. 2008). This means that  $f$  is larger than unity, due to considering the radiation pressure. The high- $f$  value is consistent with our results for NLS1s. Marconi et al. (2008) take the radiation pressure force  $F_r$  as being proportional to  $r_{\text{BLR}}^{-2}$ , and the impact of radiation pressure then is to reduce the effective black hole mass by a fixed value for all emission lines in the BLR. In contrast, we parameterise the impact of radiation pressure with a radial power-law. In the BLR model of Netzer (1990), the BLR cloud pressure is assumed to be determined by the pressure of the external medium, which has a simple power-law radial profile. Kaspi & Netzer (1999) found a good fit to the emission line responses in NGC 5548 when the external pressure (and thus also the BLR gas density) was proportional to  $r_{\text{BLR}}^{-1}$ . In such a model, the cloud

cross section  $\sigma_c$  is then proportional to  $r_{\text{BLR}}^{2/3}$ , and  $F_r$  is proportional to  $r_{\text{BLR}}^{-2}\sigma_c \propto r_{\text{BLR}}^{-4/3}$ . The effective black hole's gravity is  $F_g^{\text{eff}} = F_g - F_r = Ar_{\text{BLR}}^{-2} - Br_{\text{BLR}}^{-4/3} = Er_{\text{BLR}}^{-(2+\alpha)}$ , where  $r_{\text{BLR}}^{-\alpha}$  is the correction factor from the central disc radiation and  $\alpha > 0$ .  $Ar_{\text{BLR}}^{-2} - Br_{\text{BLR}}^{-4/3} = 0$  gives a resolution  $r_{\text{gr}}$ , and  $Er_{\text{BLR}}^{-(2+\alpha)}$  is positive for  $r < r_{\text{gr}}$ .  $F_g^{\text{eff}}$  can not be modelled as  $Er_{\text{BLR}}^{-(2+\alpha)}$  around  $r_{\text{gr}}$ . Considering the centrifugal force  $F_c$  of a cloud, there is an equilibrium point  $r_{\text{grc}}$ , and  $r_{\text{grc}}$  is smaller than  $r_{\text{gr}}$ . For comparable  $F_g$ ,  $F_r$  and  $F_c$ ,  $r_{\text{gr}}$  should be several times of  $r_{\text{grc}}$ . For BLR clouds, there are series of  $r_{\text{grc}}$ .  $F_g^{\text{eff}}$  can be effectively modelled as  $Er_{\text{BLR}}^{-(2+\alpha)}$  for these  $r_{\text{grc}}$ . Therefore, there is a ratio of  $F_g/F_g^{\text{eff}} \propto r_{\text{BLR}}^{\alpha}$ . We have  $f = M_{\bullet}/M_{\text{RM}}(f=1) = M_{\text{grav}}/M_{\text{RM}}(f=1) \propto F_g/F_g^{\text{eff}} \propto r_{\text{BLR}}^{\alpha}$ , again. At the other hand, there is  $v_c^2 \neq GM_{\bullet}/r_{\text{BLR}}$  in the presence of the radiation pressure. We have  $v_{\text{cr}}^2 = GM_{\bullet}/r_{\text{BLR}}^{1+\alpha}$  instead of  $v_c^2 = GM_{\bullet}/r_{\text{BLR}}$ . So,  $v_{\text{cr}}^2 < v_c^2$  and  $v_{\text{FWHM}}^2 \propto v_{\text{cr}}^2 \propto r_{\text{BLR}}^{-1}(r_g)r_{\text{BLR}}^{-\alpha}$ . Thus,  $f \propto r_{\text{BLR}}^{-1}(r_g)/v_{\text{FWHM}}^2 \propto r_{\text{BLR}}^{\alpha}$ , i.e.  $\log f = D + \alpha \log r_{\text{BLR}}$ , where  $D$  is independent of  $r_{\text{BLR}}$  and  $M_{\bullet}$ . The virial factor  $f$  is a function of  $r_{\text{BLR}}$  rather than  $r_{\text{BLR}}(r_g)$ . Thus, the interpretation of the effects of radiation pressure is reasonable.

Parameter  $\alpha$  is likely different from one to another AGN and might depend on accretion rate. We have  $\alpha = 0.3$  for Mrk 110 (see Figure 1). The lines parallel to the best fit line to Mrk 110 cannot connect two points of Mrk 493 or *IRAS* 04416 even considering the corresponding errors. Mrk 110, Mrk 493 and *IRAS* 04416 have  $\mathcal{M}_{f=1} = 5.89, 75.9$  and  $426.6$  or  $\mathcal{M}_f = 0.49, 1.04$  and  $7.27$ , respectively. Mrk 493 and *IRAS* 04416 have larger accretion rates than Mrk 110 and it is possible that  $\alpha$  depends on the accretion rate, but the present data do not allow us to test this hypothesis. There is a strong positive correlation between  $f$  and  $\mathcal{M}_{f=1}$ ,  $f = 6.8(\pm 1.6)\mathcal{M}_{f=1}^{0.4 \pm 0.1}$  (see Figure 3), which is consistent with  $f$  being dominated by the radiation pressure. This correlation supports the explanation of  $f = 5.4r_{\text{BLR}}^{0.3}$  in Mrk 110 arising due to the radiation pressure from the accretion disc. Thus, the relation of  $f = 6.8\mathcal{M}_{f=1}^{0.4}$  reflects the physical essence of some relations similar to  $f = 5.4r_{\text{BLR}}^{0.3}$ . The radiation pressure will produce more obvious effects on the BLR clouds as  $\alpha$  increases. As the radiation pressure vanishes,  $\alpha$  vanishes. The larger values of  $f \approx 8$ –16 make  $M_{\text{RM}}$  increase for Mrk 110. In like manner, larger  $f$  values may exist in quasars. Quasar J0100+2802 at  $z = 6.30$ , the most

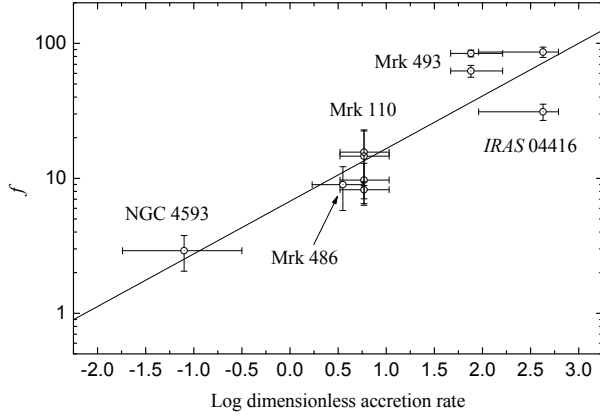


**Figure 3.**  $f$  vs  $\log \dot{M}_{f=1}$ .  $\log \dot{M}_{f=1}$  listed in Table 4. Black line is the best fit line to black circles with  $r = 0.901$  at the confidence level of 99.96 percent [ $\log y = 0.83(\pm 0.10) + 0.39(\pm 0.07) \times x$ ].

luminous quasar known at  $z > 6$ , has  $M_{\text{RM}}(f = 1) \sim 1.2 \times 10^{10} M_{\odot}$  and  $L_{\text{bol}} = 1.62 \times 10^{48} \text{ ergs s}^{-1}$  (Wu et al. 2015). It has  $L_{\text{Edd}} = 1.5 \times 10^{38} M_{\bullet}/M_{\odot} \sim 1.8 \times 10^{48} \text{ ergs s}^{-1}$  for solar composition gas and  $L_{\text{bol}}/L_{\text{Edd}} \sim 0.9$ .  $\dot{M}_{f=1} = L_{\text{bol}}/L_{\text{Edd}}/\eta$  (Du et al. 2014), where  $\eta$  is the efficiency of converting rest-mass energy to radiation (Thorne 1974) and in general  $\eta$  is on the order of 0.1. Thus  $\dot{M}_{f=1} \sim 9$  and  $f \sim 16$  for J0100+2802. As  $f \sim 16$ ,  $M_{\text{RM}} \sim 1.9 \times 10^{11} M_{\odot}$  and  $L_{\text{bol}}/L_{\text{Edd}} \sim 0.06$ . The larger black hole mass further gives rise to the most significant challenge to the Eddington limit growth of black holes in the early Universe (Volonteri 2012; Willott et al. 2010). A high- $f$  value is suggested for PG 1247+267 by the ultraviolet RM of carbon lines (Trevese et al. 2014). PG 1247+267 has  $\lambda L_{\lambda}(1350\text{\AA}) = 3.9 \times 10^{47} \text{ ergs s}^{-1}$  and ionization stratification similar to low-luminosity AGNs. The broad H $\beta$  has a redward shift of 0.008 with respect to [O III]  $\lambda 5007$  (McIntosh et al. 1999b), and has  $v_{\text{FWHM}} = 7460 \text{ km s}^{-1}$  (McIntosh et al. 1999a). If  $z_g = 0.008$ ,  $f \approx 13$ , consistent with the high- $f$  value suggested in Trevese et al. (2014). **Thus, the new method is capable of estimating  $f$  in quasars. For the Eddington ratio  $L_{\text{bol}}/L_{\text{Edd}}(f) = L_{\text{bol}}/f L_{\text{Edd}}(f = 1) = 1$ , we have  $\dot{M}_{f=1} = 1133$ ,  $f = 113$  and  $\dot{M}_f = 10$  in the case of  $\eta = 0.1$ . Then, we have  $L_{\text{bol}}/L_{\text{Edd}} = 113$  in the case of assuming  $f = 1$ . The fact that we don't often see sources with such (apparent) Eddington ratios may suggest that the Thomson cross-section typically used in the radiation pressure calculation is underestimating the coupling between the radiation and the BLR gas. If considering the line-driven radiation pressure (Castor et al. 1975), the radiation pressure due to the gas opacity will be  $\sim 10^3$  times that due to the electron scattering opacity (Ferland et al. 2009).**

With the large changes in the black hole mass estimates for these sources compared to the previous RM values, it would be interesting to know where they now fall on the  $M_{\bullet} - \sigma_{*}$  relation. We find  $\sigma_{*}$  measured by the stellar absorption lines for Mrk 110 and NGC 4593 in the literature (see Table 4). For IRAS 04416, Mrk 493 and Mrk 486, the narrow line [O III] width  $v_{\text{FWHM}}$  can be converted into  $\sigma_{*}$  by  $\sigma_{*} = v_{\text{FWHM}}/2.35$  (Nelson & Whittle 1995) (see Table

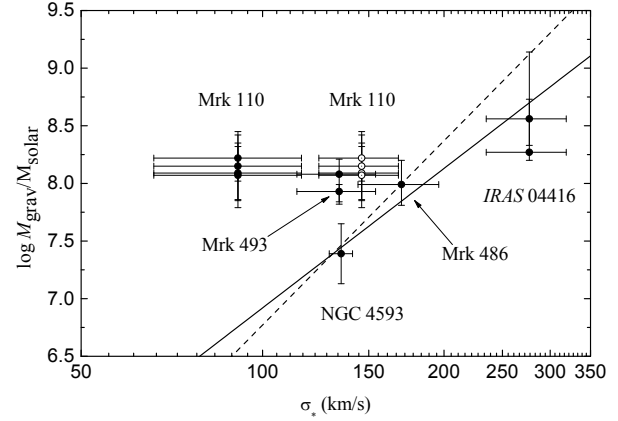


**Figure 4.**  $\log M_{\text{grav}}/M_{\odot}$  vs  $\sigma_{*}$ . Solid line is the Tremaine et al. (2002) relation for inactive galaxies. Dashed line is the Woo et al. (2013) relation for quiescent galaxies. Open circles denote  $\sigma_{*}$  converted from [O III]  $v_{\text{FWHM}}$  for Mrk 110.

4). The [O III]  $v_{\text{FWHM}}$  may serve as a good representation of  $\sigma_{*}$  (Nelson 2000), and **this method has been used in the literature** (e.g. Wang & Lu 2001).  $M_{\text{grav}}$  and  $\sigma_{*}$  are combined to show where they fall on the  $M_{\bullet} - \sigma_{*}$  relation. Since the radiation pressure can significantly influence  $f$ , we use the  $M_{\bullet} - \sigma_{*}$  relations derived for galaxies with  $M_{\bullet}$  estimated by the gas, stellar and maser kinematics. Tremaine et al. (2002) obtained for 31 nearby galaxies  $\log M_{\bullet}/M_{\odot} = 8.13 + 4.02 \log \sigma_{*}/\sigma_0$  with  $\sigma_0 = 200 \text{ km s}^{-1}$ . Woo et al. (2013) obtained for 72 quiescent galaxies  $\log M_{\bullet}/M_{\odot} = 8.37 + 5.31 \log \sigma_{*}/\sigma_0$ . The two relations are compared with the  $M_{\text{grav}}$  and  $\sigma_{*}$  of five objects. IRAS 04416, Mrk 486 and NGC 4593 follow the  $M_{\bullet} - \sigma_{*}$  relations, and **Mrk 493 is consistent with either version of the relation at better than  $2\sigma$**  (see Figure 4). However, Mrk 110 lies significantly above the two relations (see Figure 4). **Mrk 110 and Mrk 486 have nearly identical properties, with  $f$ ,  $\dot{M}_{f=1}$  and  $M_{\text{grav}}$  within the uncertainties.** So, Mrk 110 and Mrk 486 should have consistent  $\sigma_{*}$ . In fact, the  $\sigma_{*}$  of Mrk 486 is basically two times as much as that of Mrk 110. Ferrarese et al. (2001) and Nelson et al. (2004) measured  $\sigma_{*}$  for 6 and 16 Seyfert 1 galaxies by the Ca II triplet lines, respectively. **The spectra analysed by both papers have relatively low signal-to-noise ratios. The poor signal-to-noise and very shallow absorption features in Mrk 110 might lead to smaller  $\sigma_{*}$**  (see Figure 1 in Ferrarese et al. 2001). [O III]  $\lambda 5007$  has  $v_{\text{FWHM}} = 336.4 \text{ km s}^{-1}$  (Dong et al. 2011), and  $v_{\text{FWHM}} \approx 350 \text{ km s}^{-1}$  found in the SDSS DR12<sup>1</sup>. Then [O III]  $\lambda 5007$  has a mean  $v_{\text{FWHM}} \approx 343 \text{ km s}^{-1}$  and  $\sigma_{*} \approx 146 \text{ km s}^{-1}$  that makes Mrk 110 basically follow the  $M_{\bullet} - \sigma_{*}$  relations in Figure 4. In the case of high- $f$  values given by the gravitational redshift method, these five Seyfert galaxies are broadly consistent with the  $M_{\bullet} - \sigma_{*}$  relations in Figure 4. Thus, the higher  $f$  values are reasonable, and the lower black hole masses estimated in the case of  $\langle f \rangle \approx 1$  do not follow these relations.

**In some sources, blueshifted [O III]  $\lambda 5007$  emission lines have been found** (e.g. Boroson 2005;

<sup>1</sup> <http://skyserver.sdss.org/dr12/en/tools/chart/navi.aspx>

**Table 4.**  $\dot{\mathcal{M}}_{f=1}$  and  $\sigma_*$  for five Seyfert galaxies

Object (1)	$\log \dot{\mathcal{M}}_{f=1}$ (2)	$\sigma_*$ (km s $^{-1}$ ) (3)	Refs (4)
Mrk 110	$0.77^{+0.26}_{-0.25}$	$91 \pm 25^\dagger$	1
		$146 \pm 22^\ddagger$	3
NGC 4593	$-1.10^{+0.60}_{-0.64}$	$135 \pm 6^\dagger$	1
IRAS 04416	$2.63^{+0.16}_{-0.67}$	$277 \pm 42^\ddagger$	2
Mrk 493	$1.88^{+0.33}_{-0.21}$	$134 \pm 20^\ddagger$	2
Mrk 486	$0.55^{+0.20}_{-0.32}$	$170 \pm 26^\ddagger$	2

Notes: Column 1: object names; Column 2: logarithm of dimensionless accretion rate, taken from Du et al. (2015); Column 3: the stellar velocity dispersion  $\sigma_*$ ; Column 4: references of column (3). Refs 2 and 3 only give [O III]  $v_{\text{FWHM}}$ .

References: (1) Nelson et al. 2004; (2) Wang & Lu 2001; (3) the SDSS DR12.

$^\dagger$   $\sigma_*$  were measured by the stellar absorption lines.

$^\ddagger$   $\sigma_*$  are converted from [O III]  $v_{\text{FWHM}}$ , and the uncertainties are taken to be 15% of  $\sigma_*$  (e.g. Ferrarese et al. 2001).

Bae & Woo 2014; Zhou et al. 2006). The broad line shifts relative to [O III]  $\lambda 5007$  can thus acquire larger uncertainties due to the [O III] blueshifts. **Given that uncertainty in the reference redshift, it would be beneficial to avoid using [O III] as the reference for the broad line shifts.** Equation (7) only needs the redshift difference between two broad lines. Thus, the [O III] blueshifts will not influence  $M_{\text{grav}}$  given by equation (7). The consistent masses derived from equations (4) and (7) for Mrk 110 suggest that the [O III] blueshifts do not cause significant influence on  $M_{\text{grav}}$  given by equation (4) and the rms spectra. Thus, the broad-line-to-broad-line comparison path or the rms spectra could overcome the limitations of narrow line blueshifts. The mean spectra might overcome the same limitations.  $z_g$  can be given by the redward shift of the centroid of broad line with respect to its peak (Jonić et al. 2016). This approach is **another means of avoiding the limitations** of narrow line blueshifts. However, **cloud inflows could also generate a redward line shift, which could bias the gravitational redshift measurement.** Jonić et al. (2016) confirmed the gravitational redshift origin of this redward shift, **based on the theoretically expected relationship of  $\Delta z_{50} \propto v_{\text{FWHM}}^2$ .** The gravitational redshift is a natural outcome of the virialized motions of BLR clouds. The blueshifts are usual for high-ionization lines, e.g. broad C IV, and are regarded as a signal of gas outflows (e.g. Wang et al. 2011, references therein). The outflows may be driven by the radiation pressure of accretion disc. Mrk 486 has the redshifted broad Fe II and the blueshifted broad H $\beta$ . These two shifted broad lines may be explained in terms of the combination of the outflows and the gravitational redshift effect. The redshifted broad H $\beta$  and Fe II in other 3 NLS1s might be dominated by the gravitational redshift.

Müller & Wold (2006) used the Kerr ray tracing simulations to study the gravitational redshifts of Mrk 110. When  $r_{\text{BLR}} \gtrsim 100r_g$ , the simulation results for stationary rotating emitters are nearly identical to, within the errors, those for static emitters in the Kerr space-time and the Schwarzschild space-time (see Fig. 9 in Müller & Wold 2006). Mrk 110 has  $r_{\text{BLR}} \sim 560\text{--}4000 r_g$  for He II, He I,

H $\beta$  and H $\alpha$ . NGC 4593, Mrk 486, Mrk 493 and IRAS 04416 have  $r_{\text{BLR}} \sim 2700, 3100, 1700\text{--}2400$  and  $600\text{--}1300 r_g$ , respectively. So, it is reasonable to estimate  $f$  and  $M_{\text{grav}}$  by the use of formulas in section 2. IRAS 04416 and Mrk 493 have a mean  $r_{\text{BLR}} \sim 900r_g$  and  $\sim 2000r_g$ , respectively. According to Müller & Wold (2006), the gravitational redshift can be probed out to  $r_{\text{BLR}} \sim 900r_g$  and  $\sim 2000r_g$  with a resolution of  $\approx 8.3 \text{ \AA}$  and  $\approx 3.8 \text{ \AA}$ , respectively. The spectra measured in the RM campaign for SEAMBHs have a resolution of  $1.8 \text{ \AA}$  (Du et al. 2014; Hu et al. 2015). Thus,  $z_g$  can be probed out to  $r_{\text{BLR}} \sim 900r_g$  and  $\sim 2000r_g$ , respectively, for IRAS 04416 and Mrk 493 with the spectra used to measure the redward shifts of H $\beta$  and Fe II. The spectral resolution of  $\sim 500 \text{ km s}^{-1}$  mentioned in Du et al. (2014) and Hu et al. (2015) is an instrumental broadening that mainly influences width of spectrum line, such as  $v_{\text{FWHM}}$ , but slightly influences the central wavelength of spectrum line. The instrumental broadening has been corrected to obtain  $v_{\text{FWHM}}$  of broad lines in NLS1s (Du et al. 2014; Hu et al. 2015).

In this paper, based on the gravitationally redshifted optical broad emission lines in AGNs, a new method is proposed to measure the virial factors  $f$  in  $M_{\text{RM}}$  estimates by the use of  $z_g$  and  $v_{\text{FWHM}}$  of broad lines. First, this new method is applied to NLS1 Mrk 110 with the gravitationally redshifted broad lines He II, He I, H $\beta$  and H $\alpha$ . These four lines have  $f \approx 8\text{--}16$  that are distinctly larger than  $\langle f \rangle \approx 1$ . The He II and He I lines have slightly smaller  $f$  than the H $\beta$  and H $\alpha$  lines. There is a positive correlation between  $f$  and  $r_{\text{BLR}}$  for Mrk 110,  $f = 5.4r_{\text{BLR}}^{0.3}$  (see Figure 1), which can be naturally explained by the radiation pressure influence of accretion disc on the BLR clouds. The radiation pressure seems to be more important than usually thought in AGNs. Second, NGC 4593 and Mrk 486 have  $f \approx 3$  and  $f \approx 9$  given by the redward shifted H $\alpha$  and Fe II lines, respectively. Third, NLS1s Mrk 493, IRAS 04416 and Mrk 42 have high- $f$  values of several tens given by the redward shifted H $\beta$  and Fe II lines. In the plot of  $\log f$  versus  $\log r_{\text{BLR}}$ , NGC 4593 is below the best fit line to Mrk 110, Mrk 486 is around the best fit line, and both of Mrk 493 and IRAS 04416 are above the same line (see Figure 1). These differences result from the accretion rate differences. NGC 4593, Mrk 486, Mrk 110, Mrk 493 and IRAS 04416 have  $\dot{\mathcal{M}}_{f=1} = 0.08, 3.55, 5.89, 75.9$  and  $426.6$  or  $\dot{\mathcal{M}}_f = 0.03, 0.40, 0.49, 1.04$  and  $7.27$ , respectively. **We find that  $f = 6.8 \cdot \dot{\mathcal{M}}_{f=1}^{0.4}$  for these five objects (see Figure 3), which could be due to radiation pressure.** The black hole masses  $M_{\text{grav}}$  match the  $M_\bullet - \sigma_*$  relations derived from galaxies with  $M_\bullet$  estimated by the gas, stellar and maser kinematics (see Figure 4). The measurements of  $f$  by  $z_g$  of broad lines have the important potential to improve the researches on AGNs. The larger  $f$  values given by  $z_g$  **can generate higher black hole masses and lower Eddington ratios.**

## ACKNOWLEDGMENTS

We are grateful to the anonymous referee for important comments leading to significant improvement of this paper. We thank the helpful discussions of Dr. H. Q. Li, Dr. P. Du and Dr. F. Wang. HTL thanks the National Natural Science Foundation of China (NSFC; grants 11273052 and U1431228) for financial support. JMB acknowledges the



support of the NSFC (grant 11133006). HTL also thanks the financial supports of the project of the Training Programme for the Talents of West Light Foundation, CAS and the Youth Innovation Promotion Association, CAS.

## REFERENCES

- Bae H. J., Woo J. H., 2014, *ApJ*, 795, 30  
 Barth A. J. et al., 2011, *ApJ*, 743, L4  
 Barth A. J. et al., 2015, *ApJS*, 217, 26  
 Bentz M. C. et al., 2006, *ApJ*, 651, 775  
 Blandford R. D., McKee C. F., 1982, *ApJ*, 255, 419  
 Boroson T., 2005, *AJ*, 130, 381  
 Carswell R. F. et al., 1991, *ApJ*, 381, L5  
 Castor J. I., Abbott D. C., Klein R. I., 1975, *ApJ*, 195, 157  
 Denney K. D. et al., 2010, *ApJ*, 721, 715  
 Dietrich M. et al., 1994, *A&A*, 284, 33  
 Dong X. B. et al., 2011, *ApJ*, 736, 86  
 Du P. et al. (SEAMBH Collaboration), 2014, *ApJ*, 782, 45  
 Du P. et al. (SEAMBH Collaboration), 2015, *ApJ*, 806, 22  
 Du P. et al. (SEAMBH Collaboration), 2016, *ApJ*, 820, 27  
 Fabian A. C., Rees M. J., Stella L., White N. E., 1989, *MNRAS*, 238, 729  
 Fabian A. C., Iwasawa K., Reynolds C. S., Young A. J., 2000, *PASP*, 112, 1145  
 Ferland G. J. et al., 2009, *ApJL*, 707, L82  
 Ferrarese L. et al., 2001, *ApJL*, 555, L79  
 Haas M. et al., 2011, *A&A*, 535, A73  
 Hu C. et al. (SEAMBH Collaboration), 2015, *ApJ*, 804, 138  
 Jonić, S., Kovačević-Dojčinović, J., Ilić, D., Popović, L. Č., 2016, *Ap&SS*, 361, 101  
 Kaspi S., Netzer H., 1999, *ApJ*, 524, 71  
 Kaspi S. et al., 2000, *ApJ*, 533, 631  
 Kaspi S. et al., 2007, *ApJ*, 659, 997  
 King A. L. et al., 2015, *MNRAS*, 453, 1701  
 Kollatschny W., Dietrich M., 1997, *A&A*, 323, 5  
 Kollatschny W., Bischoff K., Robinson E. L., Welsh W. F., Hill G. J., 2001, *A&A*, 379, 125  
 Kollatschny W., 2003a, *A&A*, 407, 461  
 Kollatschny W., 2003b, *A&A*, 412, L61  
 Krolik J. H. et al., 1991, *ApJ*, 371, 541  
 Krolik J. H., 2001, *ApJ*, 551, 72  
 Marconi A. et al., 2008, *ApJ*, 678, 693  
 McIntosh D. H., Rieke M. J., Rix H. W., Foltz C. B., Weymann R. J., 1999a, *ApJ*, 514, 40  
 McIntosh D. H., Rix H. W., Rieke M. J., Foltz C. B., 1999b, *ApJ*, 517, L73  
 McLure R. J., Dunlop J. S., 2001, *MNRAS*, 327, 199  
 Müller A., Wold M., 2006, *A&A*, 457, 485  
 Nelson C. H., 2000, *ApJL*, 544, L91  
 Nelson C. H., Green R. F., Bower G., Gebhardt K., Weistrop D., 2004, *ApJ*, 615, 652  
 Nelson C. H., Whittle M., 1995, *ApJS*, 99, 67  
 Netzer H., 1990, in *Active Galactic Nuclei, SAAS-FEE Advanced Course 20*, ed. T. J.-L. Courvoisier & M. Mayor (Berlin: Springer), 57  
 Nishihara E. et al., 1997, *ApJ*, 488, L27  
 Onken C. A. et al., 2004, *ApJ*, 615, 645  
 Pei L. et al., 2014, *ApJ*, 795, 38  
 Peterson B. M., 1993, *PASP*, 105, 247  
 Peterson B. M. et al., 2004, *ApJ*, 613, 682  
 Peterson B. M. et al., 2005, *ApJ*, 632, 799  
 Piotrovich M. Y., Gnedin Yu. N., Silant'ev N. A., Natsvlshvili T. M., Buliga S. D., 2015, *MNRAS*, 454, 1157  
 Popovic L. C., Vince I., Atanackovic-Vukmanovic O., Kubicela A., 1995, *A&A*, 293, 309  
 Pozo Nuñez F. et al., 2012, *A&A*, 545, A84  
 Press W. H., Teukolsky S. A., Vetterling W. T., Flannery B. P. 1992, *Numerical Recipes* (2nd ed.; Cambridge: Cambridge Univ. Press)  
 Rees M. J., 1984, *ARA&A*, 22, 471  
 Rees M. J., Begelman M. C., Blandford R. D., Phinney E. S., 1982, *Nature*, 295, 17  
 Reynolds C. S., Nowak M. A., 2003, *Phys. Rep.*, 377, 389  
 Riess A. G. et al., 2004, *ApJ*, 607, 665  
 Shen Y. et al., 2015a, *ApJS*, 216, 4  
 Shen Y. et al., 2015b, *ApJ*, 805, 96  
 Shen Y. et al., 2016, *ApJ*, 818, 30  
 Spergel D. N. et al., 2003, *ApJS*, 148, 175  
 Tanaka Y. et al., 1995, *Nature*, 375, 659  
 Thorne K. S., 1974, *ApJ*, 191, 507  
 Tremaine S. et al., 2002, *ApJ*, 574, 740  
 Tremaine S., Shen Y., Liu X., Loeb A., 2014, *ApJ*, 794, 49  
 Trevese D., Perna M., Vagnetti F., Saturni F. G., Dadina M., 2014, *ApJ*, 795, 164  
 Vanden Berk D. E. et al., 2001, *AJ*, 122, 549  
 Volonteri M., 2012, *Science*, 337, 544  
 Wandel A., Peterson B. M., Makkan M. A., 1999, *ApJ*, 526, 579  
 Wang H. Y. et al., 2011, *ApJ*, 738, 85  
 Wang J. M. et al. (SEAMBH Collaboration), 2014, *ApJ*, 793, 108  
 Wang T., Lu Y., 2001, *A&A*, 377, 52  
 Willott C. J. et al., 2010, *AJ*, 140, 546  
 Woo J. H. et al., 2013, *ApJ*, 772, 49  
 Woo J. H., Yoon Y., Park S., Park D., Kim S. C., 2015, *ApJ*, 801, 38  
 Wu X. B. et al., 2015, *Nature*, 518, 512  
 Zheng W., Sulentic J. W., 1990, *ApJ*, 350, 512  
 Zhou H. Y. et al., 2006, *ApJS*, 166, 128